JOURNAL OF AIRCRAFT
Vol. 36, No. 5, September–October 1999

Hybrid Airfoil Design Procedure Validation for Full-Scale Ice Accretion Simulation

Farooq Saeed,* Michael S. Selig,† and Michael B. Bragg‡
University of Illinois at Urbana–Champaign, Urbana, Illinois 61801-2935

This paper presents results of the ice accretion tests performed to validate the hybrid airfoil design method. The hybrid airfoil design method was developed to facilitate the design of hybrid airfoils with full-scale leading edges and redesigned aft sections that simulate full-scale ice accretion simulation for a given α range. Icing tests in the NASA Lewis Icing Research Tunnel were conducted with test conditions representative of flight. A two-dimensional half-scale hybrid airfoil was designed and built with a 20% plain flap and a 5% upper and 20% lower full-scale leading-edge surface of a modern business jet wing section. This paper presents a comparison between the ice shapes accreted on the business jet and hybrid airfoil models during the tests. The test results show that ice accretion simulation could be predicted in terms of the droplet-impingement simulation alone and confirm the assumption that the leading-edge ice accretion will be the same for the full-scale and hybrid airfoils if icing cloud properties, droplet impingement, local leading-edge flowfield, model surface characteristics, and geometry are held constant. This assumption was found to be valid when tested under the most severe conditions of glaze ice accretion over a large time interval. A comparison between the actual ice shapes and those predicted by LEWICE 1.6 under similar conditions is also shown. The results suggest that the hybrid airfoil design method has significant application potential for tests where leading-edge ice accretion is desired because it provides an alternative to the myriad of issues related to ice accretion scaling.

Nomenclature

C_d = airfoil drag coefficient
C_p = pressure coefficient
c = airfoil chord length
M = freestream Mach number
P = pressure
Re = freestream Reynolds number, $\rho V_\infty c/\mu$
T = temperature
V_∞ = airspeed
x, y = airfoil coordinates
α = angle of attack relative to airfoil longest chord line, $\alpha_n - \gamma_n$
α_n = angle of attack relative to airfoil nose section
γ_n = nose droop angle
δ_f = flap deflection
μ = absolute air viscosity
ρ = air density

Subscripts

s = static
t = total
ws = wake survey

Introduction

THERE is a need within the aerospace community to better understand the process of ice accretion. This concern is due in part to icing-related accidents[1] in recent years. To improve flight safety, a better understanding of the effect of ice accretion on the aerodynamic performance of airfoils or wings is required. Because the physics of ice accretion are not well understood, computer simulations that can accurately predict the effect of ice accretion on a particular design are not currently available. Safety in icing conditions is currently ensured through the testing of aircraft with ice accretions thought to result in the largest penalties in performance and handling qualities. The determination of this critical ice accretion and its aerodynamic effect on a set of modern airfoils, typical of those in use on current aircraft, is underway at NASA John H. Glenn Research Center at Lewis Field. The research reported here is part of this larger effort.

Owing to the difficulties and uncertainties in ice accretion scaling,[2–10] testing at full scale is highly desirable. The available icing wind tunnels are, however, too small to test full-scale airfoils or wings of most aircraft of interest. Because aircraft wing ice accretion depends, primarily, on the airfoil leading-edge geometry[11] where the ice accretes, one way to expand the usefulness of existing icing tunnels and to facilitate testing of aircraft de-icing/anti-icing systems is to test hybrid airfoils or subscale airfoils. These airfoils have full-scale leading edges and redesigned aft sections to provide full-scale icing conditions at the leading edge. The term "hybrid method" refers to using a full-scale leading edge to match the full-scale ice accretion. The aft section of the hybrid airfoil is specially designed to provide a flowfield and droplet impingement similar to that on the full-scale airfoil leading edge. In an early work by Von Glahn,[12] airfoils with full-scale leading edges and truncated aft sections were used to simulate the flowfield of the full scale, thereby avoiding the associated scaling issues. Interestingly, neither the approach nor its range of application received much attention despite its numerous merits.

In the absence of a systematic study to provide insight into the design of the aft section, a study[13] was carried out in which a design procedure for hybrid airfoils was successfully developed and demonstrated with specific design examples. The formulation was based on the assumption that the leading-edge ice accretion will be the same for the full-scale and hybrid airfoils if the icing cloud properties, droplet-impingement characteristics, local nose-section flowfield, model surface geometry, model surface quality, and model surface thermodynamic characteristics are held constant. The study showed that hybrid airfoils could be designed to exhibit both the

Presented as Paper 98-0199 at the AIAA 36th Aerospace Sciences Meeting, Reno, NV, 12–15 January 1998; received 2 May 1998; revision received 3 November 1998; accepted for publication 17 December 1998.

*Graduate Research Assistant, Department of Aeronautical and Astronautical Engineering. Student Member AIAA.
†Associate Professor, Department of Aeronautical and Astronautical Engineering. Senior Member AIAA.
‡Professor, Department of Aeronautical and Astronautical Engineering. Associate Fellow AIAA.

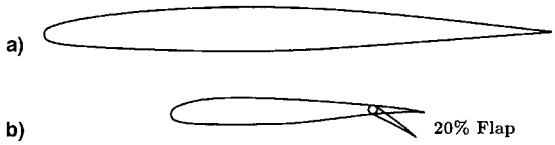

Fig. 1 Plot of a) the scaled business jet airfoil (full-scale) and b) the half-scale hybrid airfoil with a 20% flap.

full-scale flowfield on its nose section as well as full-scale droplet-impingement characteristics. The results of the study were incorporated into a hybrid airfoil design and analysis code that utilizes validated computational airfoil aerodynamics and droplet-impingement codes.[14–16]

A limitation of the design procedure presented in Ref. 13 is its restriction to single-point design, and, therefore, it lacks the capability to handle off-design cases. To overcome this limitation, a more recent study[17,18] was carried out to expand the scope of the single-point design procedure to a method that enabled the hybrid airfoils to exhibit both the full-scale local nose-section flowfield as well as droplet-impingement characteristics throughout a desired α range. The results of the study indicated that although a flap can be used very effectively to achieve full-scale droplet-impingement characteristics at off-design angles of attack α, the use of a flap does not simulate the full-scale flowfield on the nose section to an accuracy similar to that for the single-point design case. Because the difference in the local nose-section flowfield would affect the thermodynamics of ice accretion as the droplets impinge on the surface, it was suspected that ice accretion simulation may be compromised.

Hence, it became necessary to establish the validity of these methods[13,17] through extensive ice accretion tests. Thus, a series of tests were planned as part of the ongoing research effort in support of NASA's Modern Airfoil Ice Accretion program.[19] For this purpose, an airfoil similar to that found on a modern business jet main wing section, shown in Fig. 1a, was provided by NASA. The hybrid airfoil design method[13,17,18] was then used to design a half-scale hybrid airfoil (shown in Fig. 1b), such that the full-scale leading-edge geometry is maintained from 5% chord on the upper surface to 20% chord on the lower surface. The two-dimensional modern business jet and hybrid airfoil models were built at NASA Lewis Research Center for ice accretion tests in the NASA Lewis Icing Research Tunnel (IRT) for the present and a related[19] study. The icing test conditions were selected from the Federal Aviation Regulations, Part 25, Appendix C (FAR Appendix C) envelope and reflect those that a modern business jet would encounter.

The focus of this paper is to present the ice accretion test results and establish the validity of the hybrid airfoil design method[13,17,18] through a comparison of the numerical prediction and experimental results. This paper also presents a comparison of the ice shapes predicted by the NASA Lewis Research Center's ice accretion prediction code LEWICE,[20] with the experimental ice shapes. In the next section, the details of the experimental method are presented followed by a Results and Discussion section. Finally, the paper presents some important conclusions.

Experimental Methods

The experiments were performed in the IRT. Detailed information regarding the test facility can be found in Ref. 21. A brief description of the test facility and the icing tests performed to validate the hybrid airfoil design method[13,17,18] are included here.

Test Facility

The IRT is a closed-loop refrigerated wind tunnel operated by an interactive computer control system that provides monitoring and recording of test data with 500 data channels. The test section is 6 ft high, 9 ft wide, and 20 ft long. Airspeeds in the empty test section can be varied from 43.4 to 373.4 kn (50 to 430 mph). The tunnel circuit operates at or below atmospheric pressure, and the test-section total temperature range for chilled air is controlled between -20 and $+33$°F. The turbulence intensity levels vary from 0.45% at 43.4 kn (50 mph) to 0.9% at 260.4 kn (300 mph) for a dry air test.

The balance chamber encloses both the test section and control room and shares the same static pressure as the test section. An external force-balance system was used to measure aerodynamic loads on the test model. In addition to the balance, drag was also measured using a traversing wake-survey probe.

Ten spray bars containing atomizing nozzles are used to generate a uniform test-section icing cloud. The nozzles produce water droplets of median volumetric droplet diamers (MVDs) between 15 and 40 μm with liquid water content (LWC) from 0.5 to 2.5 g/m^3.

Four viewing windows (three of which are electrically heated) between the control room and the test section allow the use of photographic, video, and flow visualization equipment for recording visual data.

Model Description

The modern business jet airfoil and the hybrid airfoil models were built as two-dimensional models with a 72-in. span and fabricated specifically for vertical installation in the IRT. The two-dimensional airfoil models were mounted on the IRT 8.6-ft-diam turntable. In the sections that follow, the modern business jet main wing section is referred to as the "full-scale" airfoil. The full-scale and the hybrid models have 36-in. and 18-in. chords, respectively. (It should be noted that the 36-in. chord modern business jet airfoil is not full scale with respect to a typical business jet aircraft. Rather, the 18-in. hybrid airfoil was designed to simulate icing on the 36-in. chord airfoil model that is considered full scale for the purpose of this scaling validation experiment.) The full-scale airfoil model was fabricated as part of NASA's Modern Airfoil Ice Accretion program.[19] The same model was, therefore, utilized in the design studies[13,17,18] as well in the validation tests to save additional expense. For details regarding the full-scale business jet airfoil model, the reader is referred to Ref. 19. The details of the half-scale hybrid model are as follows.

The hybrid model was made in three separate sections: the leading edge (nose section), the main body, and a 20% chord movable flap. The leading edge, which covered 15% of the suction surface and 40% of the pressure surface, was made of fiberglass in a fashion similar to the full-scale model.[19] This was done to ensure that conduction heat transfer and surface characteristics remained the same for the two models. The main body was made of 7370 aluminum in two halves that split at the chord line of the model. This allowed the pressure instrumentation to be placed inside the model. Twenty-eight surface static pressure orifices were built into the model around its leading edge and across both surfaces of the main body. The orifices were 30 in. above the tunnel floor when installed in the IRT. The movable flap was also made of 7370 aluminum and was attached to the main body by four simple, straight, steel hinges. The small size of the flap did not allow any room for pressure instrumentation and, therefore, no pressure orifices were built into the hybrid-model flap.

A flap actuator, consisting of a rotary motor and an actuator arm, was used to deflect the flap remotely. An electric sensor was used for recording the flap deflection as well as for setting its position. Both the actuator and the sensor were attached to the turntable and they were adequately shielded from the flow.

Model Profile Accuracy

To determine the accuracy of the hybrid airfoil model profile, its digitized coordinates were compared with the coordinates of the true (design) airfoil. The comparison is shown in Fig. 2, which indicates differences in the upper (solid line) and lower (dashed line) surfaces. A displacement above or below the x axis indicates that the true coordinates lie above or below the model coordinates, respectively. Because the displacement of both lines is primarily above the axis (which is also apparent from the overlay plot in

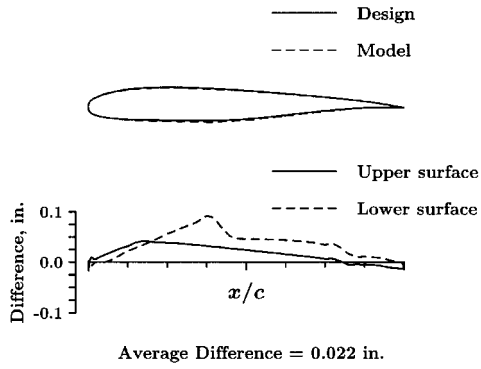

Fig. 2 Hybrid airfoil model accuracy plot (18-in. chord).

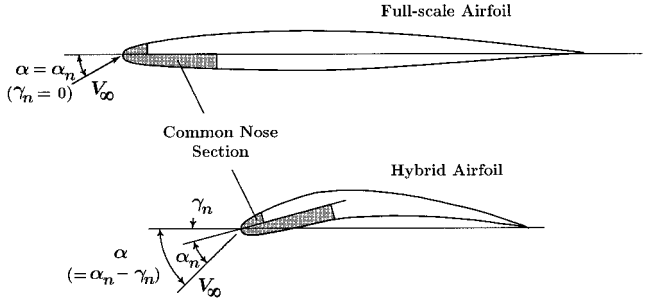

Fig. 3 Illustration of the angle-of-attack convention used in the study.

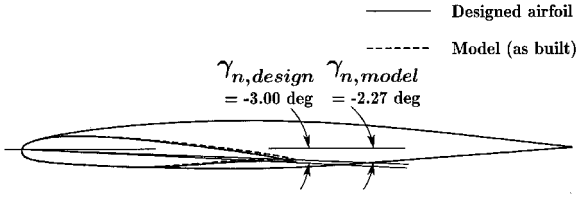

Fig. 4 Nose section overlay plot indicating the difference in the nose-droop angle.

Fig. 2), one can infer that the model airfoil has a different camber than the true airfoil. Moreover, the maximum displacements are occurring at the 15%c and 40%c locations on the upper and lower surfaces, respectively. This resulted from the leading edge or the nose section not being properly aligned with the main body of the model during installation. Overall, the average difference between the two profiles was ~0.022 in.

Figure 3 illustrates the angle-of-attack convention used in this paper. As mentioned earlier, the full-scale and the hybrid airfoil have a common nose-section geometry. The nose section of the as-designed hybrid airfoil, however, has a nose droop angle $\gamma_n = -3.00$ deg. The design philosophy[13,17,18] was to keep the nose angle of attack α_n constant and adjust the circulation with the flap to match the droplet-impingement characteristics of the full scale. Hence, the hybrid airfoil was analyzed at $\alpha = \alpha_n - \gamma_n$, where α is the angle of attack relative to the airfoil's longest chord line. Figure 4 shows the full-scale, the as-designed, and the as-built hybrid airfoil geometries such that their nose sections coincide. In this figure, the angles $\gamma_{n,\text{design}} = -3.00$ deg and $\gamma_{n,\text{model}} = -2.27$ deg represent the amount of nose droop. Figure 4 shows that the nose section of the as-built hybrid model was attached incorrectly during its construction and that the nose section is misaligned by ~0.73 deg.

As will be shown later, the misalignment of the nose section of the hybrid airfoil resulted in the disagreement between experimental data and theoretical (design) predictions. An analysis of the hybrid model (as tested) with the aid of the hybrid airfoil design code and incorporating the 0.73-deg nose misalignment shows results that are in good agreement with the experimental data.

Test Instrumentation

The wake survey system was used to measure the airfoil section drag. It consisted of a movable pitot probe that traversed the model wake at midspan and at a distance of three chords downstream of the model. The probe position was electronically sensed. Freestream conditions were measured using the facility pitot-static probe located five chords upstream of the model near the tunnel wall.

Surface pressure measurements were taken only during dry runs. Steady-state model pressures were measured using the facility's electronically scanned pressure (ESP) system.[21] The IRT has six 32-port (±5 psid) ESP modules that provide a total of 192 pressure channels, each connected to a pressure transducer that can be addressed and scanned at a rate of 10,000 ports/s. A total of 28 surface static pressure taps were built into the hybrid model as compared with 44 on the full-scale model. During the ice accretion tests the pressure taps were covered with thin tape to prevent the introduction of water into the pressure tubes.

Flow visualization was used to observe the onset of flow separation during the icing tests. Flow cones from X-Aero System, Inc., were employed for this task. A flow cone is a white plastic cone 1.75 in. long and 0.28 in. in diameter at its base. The cones were attached to the model via a 1.75-in. length of string emanating from the cone apex. A 1-in.-wide aluminum tape was applied over the string near the cone apex to attach the cone to the model. A chordwise row of cones was affixed to the model on the suction surface at ~18 in. from the tunnel floor. Video cameras were used to observe and record the movement of the cones over the model surface.

Test Conditions

The conditions used for the design of the hybrid airfoil as well as the validation tests were chosen from the FAR Appendix C envelope and are shown in Table 1. The conditions at which the actual ice accretion tests were performed are summarized in Table 2. The as-designed hybrid airfoil was designed with a nose section identical to the full-scale airfoil, but with $\gamma_n = -3$ deg. Therefore, to keep the

Table 1 Design flight and icing conditions

Variables	Full scale	Hybrid
V_∞, m/s	90	90
T_s, °C	−5	−5
Re	6×10^6	3×10^6
M	0.28	0.28
c, m	1.0	0.5
MVD, μm	20	20
α, deg	6	9
α_n, deg	6	6
γ_n, deg	0	−3

Table 2 Test conditions used in the ice accretion tests

Variables	Full scale	Hybrid
V_∞, m/s (kn)	90 (175)	90 (175)
T_s, °C (°F)	−5 (22)	−5 (22)
Re	6×10^6	3×10^6
M	0.28	0.28
LWC, g/m^3	0.54	0.54
Spray time, min	12.0	12.0
c, in.	36.0	18.0
MVD, μm	20	20
α, deg	0–8	2–11
α_n, deg	0–8	2–8
γ_n, deg	0	−3
δ_f, deg	0	−16–12

same angle of attack relative to its nose section α_n as the full-scale airfoil, the as-built hybrid airfoil was tested at $\alpha = \alpha_n - \gamma_n$. In other words, the as-built hybrid airfoil was tested at $\alpha 3$ deg higher than the corresponding full-scale test.

Test Description

A typical test run consisted of several steps. First, the model was set at the given α. After the approximate airspeed was reached, the flap was set to the desired position. The tunnel airspeed was adjusted to account for the change due to flap deflection. Then, the tunnel air was brought to the desired operating temperature. Next a wake survey was taken to measure the clean airfoil drag. The model was then subjected to the desired icing conditions for the specified amount of time. After the icing cloud was terminated, another wake survey was taken and recorded. The tunnel fan was then brought to a stop such that detailed records of the ice shape could be made.

Photographs of the accreted ice were taken with a 35-mm camera. Then the ice was cut, using a warm aluminum template, in three spanwise locations—30 in., 36 in., and 42 in. from the floor—so that hand tracings using a pencil and cardboard template could be made of the ice-shape profile. The ice thickness was measured at each of these cuts using a depth gauge. Typically, two ice-depth measurements were made at each cut: a suction surface maximum and a pressure surface maximum ice thickness. The ice was then cleaned off the model and the tunnel cleared for the next test run.

Results and Discussion

A total of 49 ice accretion tests were conducted for this study, which included 11 ice accretion tests on the full-scale (business jet) airfoil model. In addition, surface pressure measurement tests were also conducted on the hybrid model as well. Surface pressure data for the full-scale model were taken as part of NASA's Modern Airfoil Ice Accretion program.[19] The data presented here have been restricted to the results that are pertinent to the validation of the hybrid airfoil design method.[13,17,18] Therefore, only the significant ice shape data have been included in this paper.

First, the repeatability and accuracy of the experimental results are discussed. Then the hybrid model ice shapes are shown in comparison with the full-scale model ice shapes to determine the flap deflection that best simulates the full-scale ice accretion. The optimum flap deflection is determined for each angle-of-attack case and is then compared with the theoretical predictions. Results from the NASA Lewis Research Center's ice accretion code LEWICE[20] are also presented and compared with the experiment.

As mentioned earlier, the misalignment of the hybrid-airfoil nose section resulted in a disagreement between experimental data and theoretical predictions. However, an analysis of the hybrid model (as tested) with the aid of the hybrid airfoil design code showed that, in fact, the disagreement was due to the misalignment of the nose section that led to an incorrect interpretation of the angle-of-attack values reported in the tests. A correction to the angle-of-attack values yielded results that are in good agreement with the experimental data.

Experimental Repeatability and Accuracy

Several icing tests were conducted to determine the repeatability of the ice shapes and the corresponding drag forces based on the wake survey data. In this paper, the repeat cases are represented by the run numbers followed by the letter "r" and a repetition number. Figures 5a and 5b show a comparison of the ice-shape tracings from separate icing test runs under similar test conditions for the full-scale and the hybrid models, respectively. In general, the repeatability of ice shapes was observed to be as good as shown in Fig. 5a. Reference 22 indicates that the amount of ice shape variability, as shown in Fig. 5a, is typical. A few cases, such as run 501 in Fig. 5b, were, however, also encountered.

Repeatability of the section drag coefficients, as measured by the wake survey system, was also found to be good (within ±5%). The results for the test cases of Fig. 5a are shown in Fig. 6. Figure 7 shows

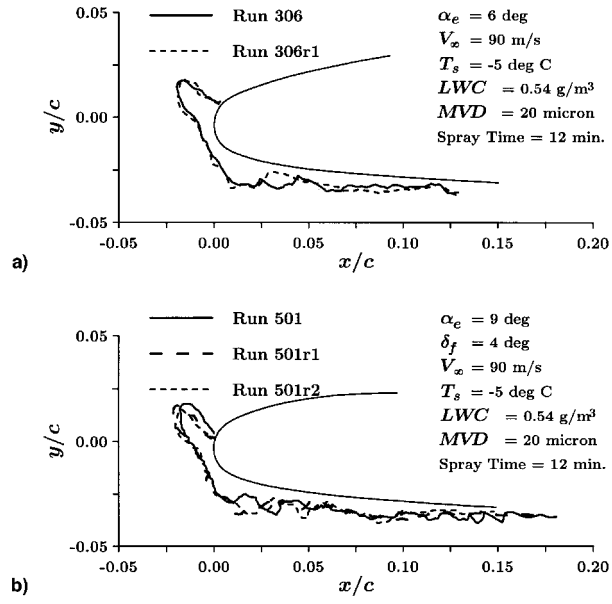

Fig. 5 Ice-shape repeatability in the IRT for a) the full-scale model and b) the hybrid model.

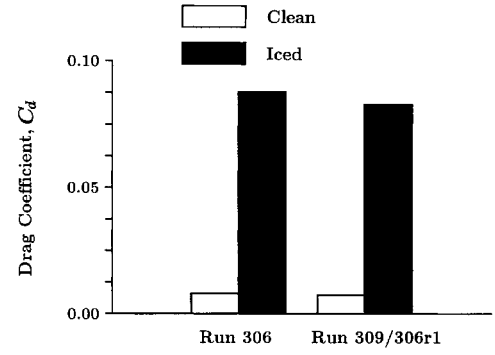

Fig. 6 Repeatability of section drag coefficient for separate test runs before and after ice accretion (test conditions shown in Fig. 5a).

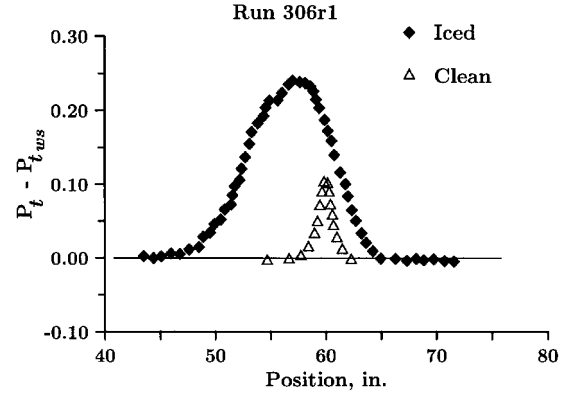

Fig. 7 Comparison of the size of the wake profiles of the clean and iced full-scale airfoil (test conditions shown in Fig. 5a).

a comparison of the total pressure deficit in the wake between the clean and iced full-scale airfoil for the same test conditions. As is obvious from Fig. 7, the ice accretion can have a tremendous effect on the size of the airfoil wake.

Experimental Ice Shapes

The experimental ice-shape tracings are shown in Figs. 8a–8d for different angle-of-attack conditions. The figures show the effectiveness of a flap in varying the ice accretion, and therefore, indicate its usefulness in simulating full-scale ice accretions. As evident from these results, the ice shapes were sensitive even to small changes (±2 deg) in the flap deflection. An explanation of the results can be given in terms of the airfoil circulation.

The amount of circulation, which was governed by both the angle of attack and flap deflection, played a dominant role in determining

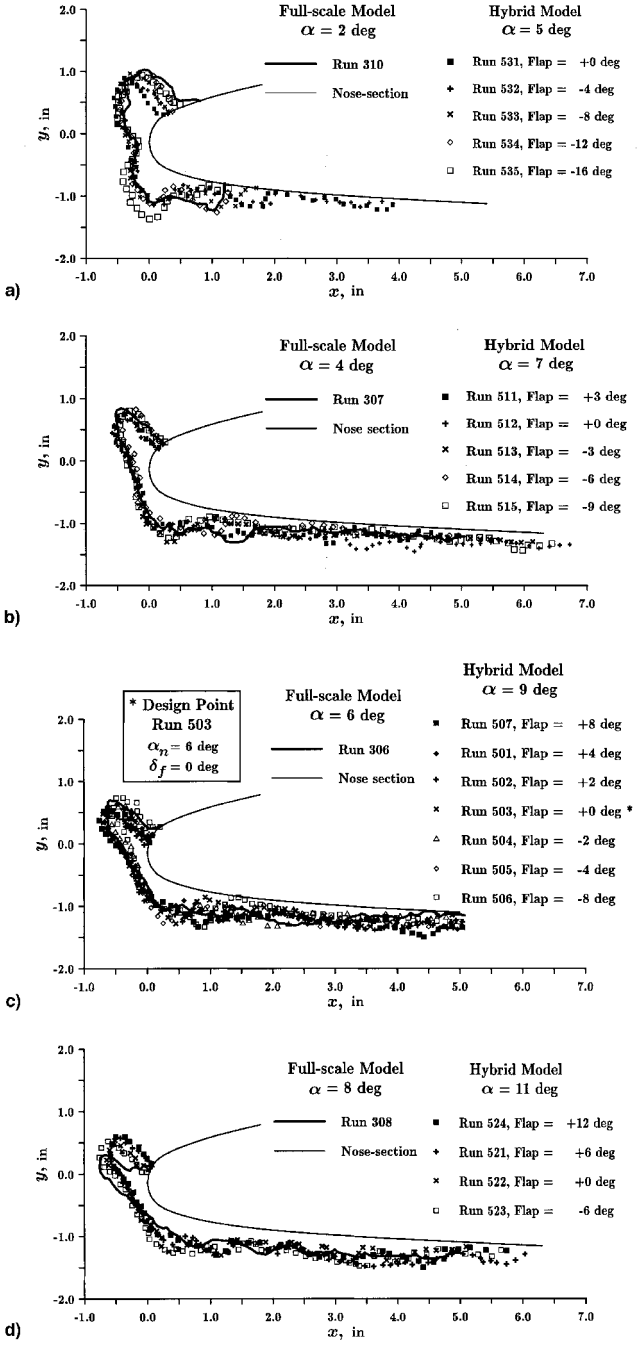

Fig. 8 Comparison of full-scale and hybrid airfoil ice shapes at several angles of attack and at test conditions: $T_s = -5°C$, MVD = 20 μm, LWC = 0.54 g/m^3, V_∞ = 90 m/s, and spray time = 12 min.

the impingement characteristics through its impact on the flowfield, and therefore, the ice accretion. In Figs. 8a–8c, an increase in flap deflection resulted in an increase in circulation as seen by the upper surface limit of the accreted ice mass that was displaced toward the leading edge. In Fig. 8d, the opposite was true, which indicates an already stalled hybrid airfoil, because a decrease in flap deflection caused the upper extent of ice accretion to move forward signifying increased circulation.

Figure 9 shows the plot of hybrid airfoil ice shapes that best simulate the corresponding full-scale airfoil ice shapes for the specified test conditions. This has been shown to indicate the optimum flap deflection on the hybrid airfoil. The design point depicted on Fig. 9c indicates that the test conditions for those tests correspond to the design point for the hybrid model.

Ice-Shape Prediction Using LEWICE

LEWICE[20] is an ice accretion prediction code that uses a time-stepping procedure to determine the shape of the ice accretion. LEWICE Version 1.6 was run to determine the usefulness of the code in the hybrid airfoil design process. The LEWICE code was run with the IRT tunnel conditions, the geometry of the as-built model (the coordinates were smoothed with the aid of XFOIL), and input flags that allowed control over the number of time steps to be used for simulation. Specifically, the IFLO (number of time steps)[20] parameter was set equal to 4 in all the cases reported in this paper on the basis of a parametric study that showed that IFLO = 4 produced results that were more consistent with experiments. For details regarding important parameters and other features of the LEWICE code, the reader is referred to the most recent update to the User's Manual.[20]

The full-scale and hybrid model airfoil (as tested) were analyzed using the LEWICE code to determine the optimum flap deflections on the hybrid airfoil that best simulate the full-scale predicted ice shapes for a given test condition. Some of the significant results are shown in Fig. 10, which is similar to Fig. 9, except that in Fig. 10 the results from the LEWICE code have also been included for comparison with the experiment.

The results from the LEWICE code shown in Fig. 10 are the cases that best simulate the predicted full-scale ice shapes. The experimental data are also shown in the figure and it is encouraging to note that the LEWICE code predicts optimum flap deflections that are in good agreement with the observed values for low-to-moderate angles of attack (below $\alpha = 11$ deg). This is true in spite of the fact that the predicted ice shapes are quite different than the experimental shapes. At this time the LEWICE code is not always able to accurately predict glaze or mixed ice accretions such as those of the test conditions that were selected for the present study.

Flow and Droplet Impingement Analysis of the Hybrid Model Airfoil

As evident from Fig. 4, the as-designed and as-built hybrid airfoils have nose-droop angles $\gamma_{n,\text{design}} = -3$ deg and $\gamma_{n,\text{model}} = -2.27$ deg, respectively. The lower value of the as-built hybrid airfoil nose-droop angle is a result of the misalignment of its nose section, and indicates that the as-built (model) hybrid airfoil has a lower camber than the as-designed hybrid airfoil. This fact was confirmed by a droplet-impingement analysis of the as-built hybrid airfoil using the hybrid airfoil design and analysis code.[17,18]

In Fig. 11a, the flap deflection δ_f required to match the full-scale ice accretion vs hybrid model angle of attack α is shown. The numerical prediction on the figure has been generated in two different ways to account for the as-built hybrid model geometry. In Fig. 11a, numerical simulation was used to predict δ_f when α_n was matched, which required that the hybrid model be run at a lower α than designed. The results show a shift between experimental data and numerical predictions when α_n was held constant. Because of the misalignment of the nose section, the model airfoil not only has a lesser camber, but is also at a lower α (by approximately $\gamma_{n,\text{design}} - \gamma_{n,\text{model}} = -0.73$ deg) when the two nose sections are aligned with the flow.

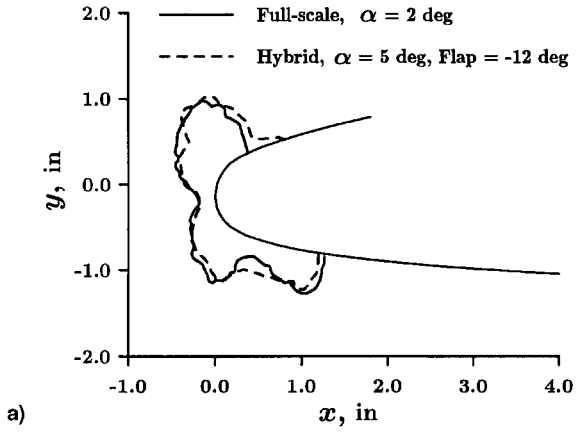

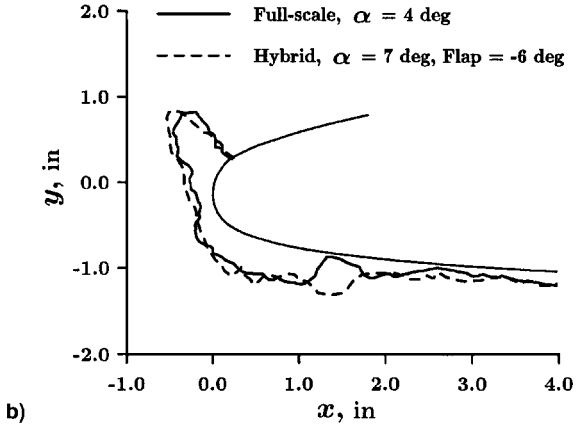

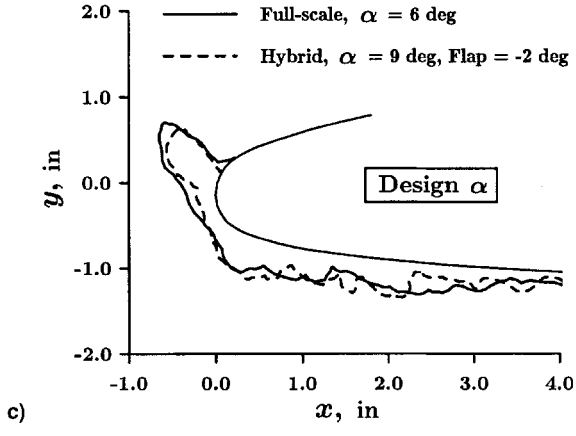

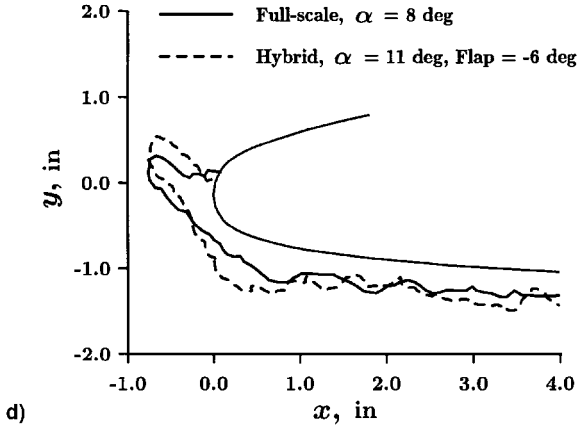

Fig. 9 Plot of hybrid airfoil ice shapes that best simulate the corresponding full-scale ice shapes for the test conditions: $T_s = -5°C$, MVD = 20 μm, LWC = 0.54 g/m^3, V_∞ = 90 m/s, and spray time = 12 min.

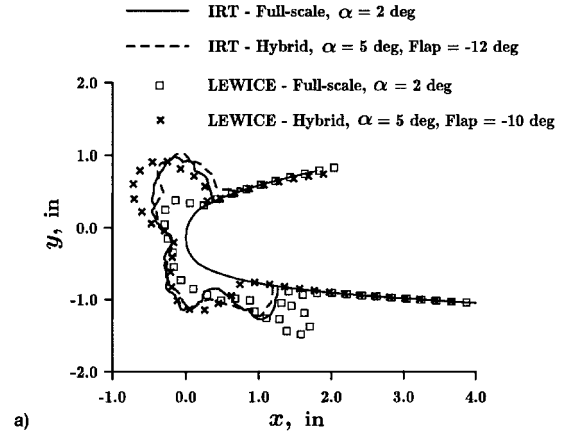

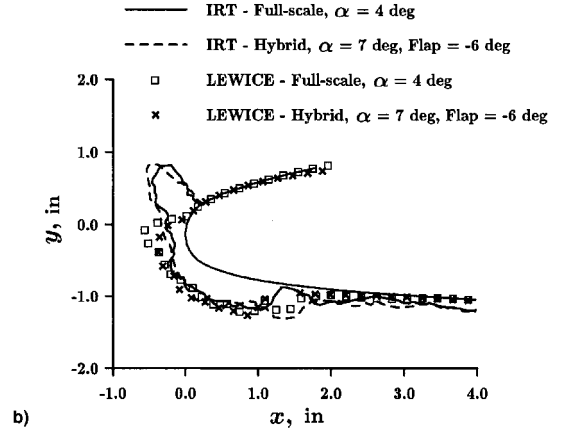

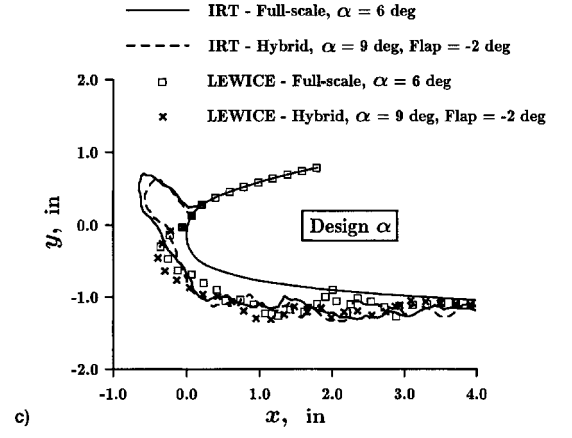

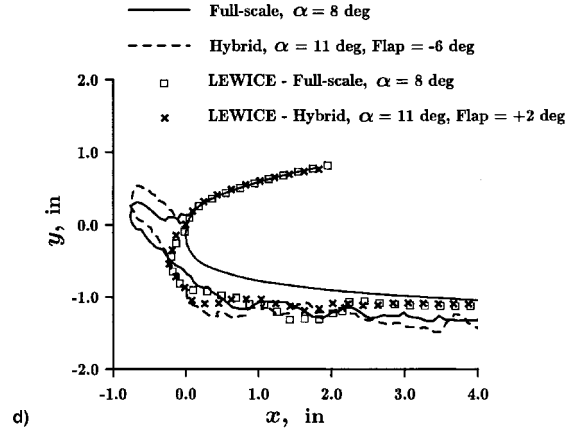

Fig. 10 Comparison of actual ice shapes with LEWICE predictions for the test conditions: $T_s = -5°C$, MVD = 20 μm, LWC = 0.54 g/m^3, V_∞ = 90 m/s, and spray time = 12 min.

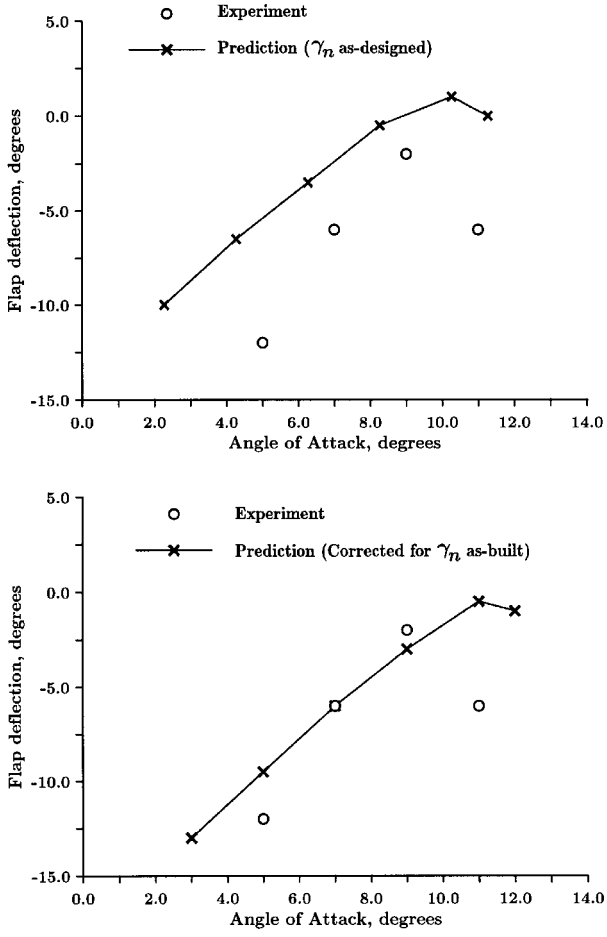

Fig. 11 Plot of the optimum flap deflection from different analyses in comparison with IRT tests data. Numerical predictions a) uncorrected and b) corrected for angles of attack.

To account for the loss of camber and insufficient nose-droop angle, a droplet-impingement analysis of the as-built hybrid airfoil was performed at an α 0.73 deg higher than that of the corresponding full-scale case. This corresponds approximately to holding α constant between the models. The results, shown in Fig. 11b, now show good agreement with the experimental data because, at a higher angle of attack, the hybrid airfoil requires a more negative value of flap deflection to account for the increase in circulation. The results show that it is possible to simulate full-scale ice accretion using subscale hybrid airfoils with plain flaps and that the design theory can accurately predict the δ_f required.

These results are, however, based on a limited number of ice accretion tests in which the only variable was the angle of attack. A more extensive test program that involves the study of the effect of other design variables, such as droplet size, temperature, speed, etc., on the design is needed to fully validate the current method.

Conclusions

Several important observations can be drawn from the validation tests. The most important, however, is that hybrid airfoils can be used to simulate full-scale ice accretion over a range of angle of attack. The icing tests confirm an important assumption of the hybrid airfoil design method that the leading-edge ice accretion will be the same between the full-scale and hybrid airfoils if icing cloud properties, droplet impingement, local leading-edge flowfield, model surface geometry, model surface quality, and model surface thermodynamic characteristics are held constant. This assumption was found to be valid when tested under the most severe conditions of glaze ice accretion over a large time interval.

Because of the as-built model geometry, the design requirements that both the full-scale and hybrid airfoil nose sections should be aligned at the same angle of attack α_n was relaxed, and yet good ice shape similitude was obtained. This suggests that this requirement may be relaxed under some conditions that could increase the applicability of the method to a large range of conditions.

The results show the usefulness of a flap system in simulating full-scale droplet-impingement characteristics as well as ice accretions. The results, however, suggest that the use of flap should be restricted to low and moderate angles of attack, because at high absolute angles of attack together with high flap deflections, the hybrid airfoils become susceptible to flow separation. This limitation could be overcome by the use of a more sophisticated flap system, by the application of boundary-layer control methods, or by relaxing the constant α_n requirement as discussed earlier.

The results from the initial series of validation tests are encouraging and suggest that the method has great application potential and that it provides an alternative to icing scaling laws. The method could be combined with traditional icing scaling methods to reduce the overall scale of the test models.

Acknowledgments

This work has been sponsored by NASA John H. Glenn Research Center at Lewis Field under Grant NCC3-408. The authors are indebted to Harold E. Addy, Jr., of the Center for supervising and conducting the experimental work without which this study would not have been accomplished. Helpful discussions with Tom Ratvasky and Tom Bond, also of the Center, are gratefully acknowledged. We would like to thank Dave Sheldon and the IRT staff for their valuable advice and assistance throughout the ice accretion tests. Also, we would like to thank William Wright for his guidance in the use of the Center's LEWICE code.

References

[1]Bragg, M. B., "Aircraft Aerodynamic Effects Due to Large Droplet Ice Accretions," AIAA Paper 96-0932, Jan. 1996.

[2]Hauger, H. H., and Englar, K. G., "Analysis of Model Testing in an Icing Wind Tunnel," Douglas Aircraft, Rept. SM 14993, Long Beach, CA, May 1954.

[3]Sibley, P. J., and Smith, R. E., Jr., "Model Testing in an Icing Wind Tunnel," Lockheed Aircraft, Rept. LR 10981, Palmdale, CA, Oct. 1955.

[4]Dodson, E. D., "Scale Model Analogy for Icing Tunnel Testing," Boeing Airplane, Transport Div., Document D66-7976, Seattle, WA, March 1962.

[5]Bragg, M. B., Gregorek, G. M., and Shaw, R. J., "An Analytical Approach to Airfoil Icing," AIAA Paper 81-0403, Jan. 1981.

[6]Ruff, G. A., "Verification and Application of the Icing Scaling Equations," AIAA Paper 86-0481, Jan. 1986.

[7]Bilanin, A. J., "Proposed Modifications to Ice Accretion/Icing Scaling Theory," AIAA Paper 88-0203, Jan. 1988.

[8]Anderson, D. N., "Rime-, Mixed- and Glaze-Ice Evaluations of Three Scaling Laws," AIAA Paper 94-0718, Jan. 1994; also NASA TM 106461, Jan. 1994.

[9]Anderson, D. N., "Methods for Scaling Icing Test Conditions," AIAA Paper 95-0540, Jan. 1995; also NASA TM 106827, Jan. 1995.

[10]Anderson, D. N., "Further Evaluation of Traditional Icing Scaling Methods," AIAA Paper 96-0633, Jan. 1996; also NASA TM 107140, Jan. 1996.

[11]Bragg, M. B., "Effect of Geometry on Airfoil Icing Characteristics," *Journal of Aircraft*, Vol. 21, No. 7, 1984, pp. 505–511.

[12]Von Glahn, U. H., "Use of Truncated Flapped Airfoils for Impingement and Icing Tests of Full Scale Leading-Edge Sections," NACA RM E56E11, July 1956.

[13]Saeed, F., Selig, M. S., and Bragg, M. B., "Design of Subscale Airfoils with Full-Scale Leading Edges for Ice Accretion Testing," *Journal of Aircraft*, Vol. 34, No. 1, 1997, pp. 94–100; also AIAA Paper 96-0635, Jan. 1996.

[14]Bragg, M. B., "Rime Ice Accretion and Its Effect on Airfoil Performance," Ph.D. Dissertation, Dept. of Aeronautical and Astronautical Engineering, Ohio State Univ., Columbus, OH, 1981; also NASA CR 165599, March 1982.

[15]Drela, M., "XFOIL: An Analysis and Design System for Low Reynolds Number Airfoils," *Lecture Notes in Engineering: Low Reynolds Number Aerodynamics*, edited by T. J. Mueller, Vol. 54, Springer–Verlag, New York, 1989, pp. 1–12.

[16]Selig, M. S., and Maughmer, M. D., "A Multipoint Inverse Airfoil Design Method Based on Conformal Mapping," *AIAA Journal*, Vol. 30, No. 5,

1992, pp. 1162–1170.

[17] Saeed, F., Selig, M. S., and Bragg, M. B., "Hybrid Airfoil Design Method to Simulate Full-Scale Ice Accretion Throughout a Given α Range," *Journal of Aircraft*, Vol. 35, No. 2, 1998, pp. 233–239; also AIAA Paper 97-0054, Jan. 1997.

[18] Saeed, F., "Hybrid Airfoil Design Methods for Full-Scale Ice Accretion Simulation," Ph.D. Dissertation, Dept. of Aeronautical and Astronautical Engineering, Univ. of Illinois at Urbana–Champaign, Urbana, IL, Jan. 1999.

[19] Addy, H. E., Jr., Potapczuk, M. G., and Sheldon, D. W., "Modern Airfoil Ice Accretions," NASA TM 107423, March 1997; also AIAA Paper 97-0174, Jan. 1997.

[20] Wright, W. B., "User Manual for the Improved NASA Lewis Ice Accretion Code LEWICE 1.6," NASA CR 198355, June 1995.

[21] Soeder, R. H., Sheldon, D. W., Andracchio, C. R., Ide, R. F., Spera, D. A., and Lalli, N. M., "NASA Lewis Icing Research Tunnel User Manual," NASA TM 107159, June 1996.

[22] Shin, J., and Bond, T. H., "Repeatability of Ice Shapes in the NASA Lewis Icing Research Tunnel," *Journal of Aircraft*, Vol. 31, No. 5, 1994, pp. 1057–1063.